Ecotoxicology and Environmental Safety 303 (2025) 119030

Contents lists available at ScienceDirect

Ecotoxicology and Environmental Safety

journal homepage: www.elsevier.com/locate/ecoenv

Vacuum ultraviolet-induced degradation of polyethylene and polyvinyl chloride micro/nanoplastics enhances their cytotoxicity and lipid peroxidation level

Sota Manabe [a], Yuya Haga [a,b,*], Hirofumi Tsujino [a,b,c], Yudai Ikuno [b], Wakaba Idehara [a], Mii Hokaku [a], Phyo Bo Bo Aung [b], Haruyasu Asahara [a,b,d], Kazuma Higashisaka [a,b,e], Yasuo Tsutsumi [a,b,d,f,g,h,*]

[a] School of Pharmaceutical Sciences, The University of Osaka, 1-6 Yamadaoka, Suita, Osaka 565-0871, Japan
[b] Graduate School of Pharmaceutical Sciences, The University of Osaka, 1-6 Yamadaoka, Suita, Osaka 565-0871, Japan
[c] Museum Links, The University of Osaka, 1-13 Machikaneyamacho, Toyonaka, Osaka 560-0043, Japan
[d] Institute for Open and Transdisciplinary Research Initiatives, The University of Osaka, 1-1 Yamadaoka, Suita, Osaka 565-0871, Japan
[e] Institute for Advanced Co-Creation Studies, The University of Osaka, 1-6 Yamadaoka, Suita, Osaka 565-0871, Japan
[f] Graduate School of Medicine, The University of Osaka, 2-2 Yamadaoka, Suita, Osaka 565-0871, Japan
[g] Global Center for Medical Engineering and Informatics, The University of Osaka, 2-2 Yamadaoka, Suita, Osaka 565-0871, Japan
[h] R3 Institute for Newly-Emerging Science Design, The University of Osaka, 1-3 Machikaneyamacho, Toyonaka, Osaka 560-8531, Japan

ARTICLE INFO

Edited by Guorui Liu

Keywords:
Reactive oxygen species
Surface degradation
Macrophage
Cell death mechanism
Toxicity assessment

ABSTRACT

Plastic particles smaller than 5 mm, termed microplastics, have raised concerns regarding their potential impact on human health. Even smaller particles (<1 μm), classified as nanoplastics, also warrant further investigation. Since these plastic particles have been detected in various human tissues, their biological effects must be thoroughly evaluated. These plastics originate from diverse polymer types and exhibit complex physicochemical properties such as size, shape, and surface degradation in the environment. However, current studies mainly utilize polystyrene beads, which may not exist widely in the environment. Therefore, the use of environmentally relevant micro- and nanoplastics for safety assessments is crucial. Focusing mainly on surface degradation, this study aimed to elucidate detailed mechanisms of cell death caused by micro- and nanoplastics and assess their universality across different polymer types, including polyethylene (PE) and polyvinyl chloride (PVC). Surface-degraded samples of PE and PVC with different particle sizes, including microplastics and nanoplastics, were prepared and their cell death mechanisms were evaluated in murine macrophage RAW264.7 cells. Transcriptomic analysis revealed that degraded PE microplastics upregulated ferroptosis-related gene expressions and increased reactive oxygen species level and lipid peroxidation. Cell death and lipid peroxidation induction were also examined in other polymer types, including PVC microplastics as well as PE and PVC nanoplastics. Notably, only the degraded samples induced cell death and lipid peroxidation for all tested particles. Given the role of lipid peroxidation in various diseases such as neurological dysfunction and ischemia-reperfusion injury, our findings highlight the potential health risks of environmental micro- and nanoplastics.

1. Introduction

Plastic litter is a pressing global issue, emphasized under SDG 14, "Protecting the Marine Environment." Plastic usage has surged from 2 million tons in 1950–380 million tons in 2015 and has been estimated to exceed 2.5 billion tons by 2050 (Geyer et al., 2017a). Owing to their low recycling rates and potential to act as carriers of harmful substances such as persistent organic pollutants, concerns regarding their negative biological and ecological effects have intensified (Okoye et al., 2022).

Plastic waste released into the environment is gradually broken down into smaller fragments through processes such as degradation and physical abrasion. Regarding these particles, microplastics (MPs) are defined as plastic particles smaller than 5 mm, while those smaller than 1 μm are referred to as nanoplastics (NPs) (Gigault et al., 2018). MPs and

* Correspondence to: Graduate School of Pharmaceutical Sciences, Osaka University, 1-6, Yamadaoka, Suita, Osaka 565-0871, Japan.
E-mail addresses: haga-y@phs.osaka-u.ac.jp (Y. Haga), ytsutsumi@phs.osaka-u.ac.jp (Y. Tsutsumi).

https://doi.org/10.1016/j.ecoenv.2025.119030
Received 28 April 2025; Received in revised form 4 September 2025; Accepted 7 September 2025
Available online 10 September 2025

NPs (collectively termed MNPs) were generated in the environment or intentionally manufactured (Thompson et al., 2004). MNPs have been detected throughout the environment, including in the atmosphere and freshwater and marine ecosystems (Kye et al., 2023; Trainic et al., 2020). MNPs have also been detected in consumable items such as salt (Karami et al., 2017) and drinking water (Koelmans et al., 2019), indicating potential human ingestion. MPs contamination in drinking water has been reported globally, highlighting its widespread presence in everyday environments (Agbasi et al., 2025). This issue is not confined to specific regions but represents a global environmental concern (Sources and Environmental Distribution of Microplastics in Nigeria, 2024; Modeling of Modeling of Modeling of Microplastic Contamination Using Soft Computational Methods, 2024). In response, numerous studies have focused on elucidating transport pathways and developing effective remediation strategies (A Review on Microplastics Migration from Sources Through Wastewater to the Environments, 2024; The Nexus Between the Transport Mechanisms and Remediation Techniques of Microplastics, 2024). Despite these efforts, the global quantity of MPs continues to increase (Belioka and Achilias, 2024). Most importantly, MNPs have been reported from human tissues, including the placenta (Ragusa et al., 2021), lungs (Jenner et al., 2022), brain (Amato-Lourenço et al., 2024), intestine, (Ibrahim et al., 2021) and blood (Leslie et al., 2022), suggesting widespread human exposure. Recent studies have suggested a correlation between MNP presence in the body and disease status, such as inflammatory bowel disease (IBD) (Yan et al., 2022) and cardiovascular events (Marfella et al., 2024).

Given the detection of MNPs in human tissues and their potential association with various diseases, alongside possible exposure pathways such as ingestion, inhalation, and dermal contact, it is crucial to investigate the effects of MNPs on human health (Toxicological Effects of Ingested Microplastics on Human Health, 2024). Such assessments must consider the diverse physicochemical properties of MNPs in the environment, including variations in particle size, shape, and surface degradation (Lambert et al., 2017; Lim, 2021a). Surface degradation is a key characteristic of environmental MNPs. It refers to the chemical modifications of the particle surface—introduction of oxygen-containing functional groups onto the surface—induced by ultraviolet (UV) light and oxygen (Alimi et al., 2022). To accurately evaluate the biological effects of MNPs, it is essential to incorporate their physicochemical properties into toxicity assessments. Although recent studies have primarily focused on polystyrene (PS) particles (Thompson et al., 2024; De Ruijter et al., 2020), it has not adequately addressed the potential impacts of polymer materials other than PS (Lim, 2021b). Furthermore, many of these studies utilize samples with uniform material composition, size, and shape (Lim, 2021a; Alimi et al., 2022), frequently neglecting surface degradation and other environmentally relevant transformations (Lambert et al., 2017). Therefore, while studying MNP toxicity, their diverse environmental properties, including the impact of surface degradation, should also be taken into account.

In our previous study, MNP samples mimicking environmental surface properties were previously prepared using vacuum ultraviolet (VUV) light irradiation and assessed their biological effects (Manabe et al., 2024; Ikuno et al., 2023, 2024a). The VUV-based degradation method at 172 nm enables rapid processing and has been demonstrated to produce surface degradation levels comparable to those observed in environmentally weathered samples (Ikuno et al., 2024a). In addition, Polyethylene (PE) microplastics with surface degradation (dPE-MP), exhibiting a degradation level comparable to that observed in the environment, were found to exhibit stronger cytotoxicity than undegraded PE-MP, inducing programmed cell death beyond apoptosis (Manabe et al., 2024). However, underlying cell death mechanisms are not fully understood. The present study aimed to explore the biological mechanisms underlying the cytotoxicity of dPE-MPs and investigate whether similar effects are observed with other polymer types or sizes formed by VUV degradation, focusing on lipid peroxidation as a potential mechanism.

2. Materials and methods

2.1. MP/NP degradation

In this study, flo-thene (Sumitomo Seika Chemicals Company, Osaka, Japan) with medium particle size 230 μm (Ikuno et al., 2024b) was used as the PE particle sample and polyvinyl chloride (PVC) powder sample (Fujifilm Wako Pure Chemicals Corporation, Osaka, Japan) with a particle size of around 100 μm was used as PVC-MP. The degradation of PE and PVC was performed following previously established protocols that demonstrated effective degradation of PE (Ikuno et al., 2023, 2024a). Briefly, to degrade PE and PVC, a FLAT EXCIMER EX-mini (Hamamatsu Photonics K. K., Shizuoka, Japan) to irradiate UV light with a wavelength of 172 nm with an intensity of 50 mW/cm^2 in the range of 86 × 40 mm was used. First, the PE or PVC sample was spread on the bottom of a Petri dish, which was placed approximately 10 mm from the light source and irradiated with UV light for 30 min. The treated PE and PVC samples were collected in a sample bottle.

To confirm PE/PVC degradation, attenuated total reflection infrared (ATR-IR) spectra were measured using the FT/IR-4700 spectrophotometer (Jasco, Tokyo, Japan) with a TGS detector. A diamond ATR crystal (incident angle of 45°, approximately one reflection) set in a horizontal ATR accessory was used to analyze the sample. All spectra were collected with 32 scans at 4 cm^{-1} resolution in the 4000–500 cm^{-1} range. First, the background spectrum was measured with no sample placed on the ATR crystal (air). The PE or PVC sample was then placed on the ATR crystal and pressed, and the IR spectra of the samples were recorded immediately. The raw spectra are presented as the pATR (= −log I/I$_0$) spectra, where the sample spectral intensity I was divided by the background spectral intensity I$_0$ just before the sample measurement.

2.2. Carbonyl index (CI)

CI is commonly used to evaluate the degree of degradation of MNPs (Almond et al., 2020). In this study, this index was obtained by evaluating the ratio of the heights of the peaks corresponding to C═O bonds (1714 cm^{-1}) and C–H bonds (1464 cm^{-1}) for PE. Similarly, for PVC, the ratio of the heights of the peaks corresponding to C═O (1724 cm^{-1}) and CH_2 bonds (1426 cm^{-1}) were considered. The ATR-IR spectra of PE before and after VUV exposure (Supplementary Figs. 1B and 3 C) demonstrated a transition in chemical structure. The characteristic CH_2 bending band at 1464 cm^{-1} was observed prior to irradiation, while a new peak appeared at 1714 cm^{-1} following VUV treatment, indicating the introduction of carbonyl groups and confirming surface oxidation. In the case of PVC (Supplementary Figs. 2B and 3 F), a similar spectral change was observed, with the appearance of a C═O stretching band at 1724 cm^{-1} in addition to the existing CH_2 band at 1426 cm^{-1} . In both cases, arrows were added to the supplementary figures to clearly indicate the relevant spectral bands used in the CI calculation. Our method was previously validated by comparing the CI values of VUV-treated PE with those of environmentally weathered PE-MP (Ikuno et al., 2024a), demonstrating comparable levels of degradation.

2.3. Preparation of PE-NP and PVC-NP

NPs were prepared according to a previous report (Tanaka et al., 2021). Briefly, 8 mg of PE-MP and 12 mg of PVC-MP were weighed and placed in a glass test tube with a lid. PE-MP was dissolved in 4 mL of xylene while PVC-MP was dissolved in 3 mL of cyclohexanone. A mixture of 100 mL DMSO (PE) or mixture of 65 mL DMSO and 35 mL water (PVC) was placed in a heat-resistant container with a stirrer and heated using a hot stirrer. After 2.5 h when the temperature reached 110–115°C (PE) or 40–42°C (PVC), the polymer solution was added to

the DMSO solution at a constant rate using a Pasteur pipette. After cooling the heat-resistant vessel in room temperature water, the solution was passed through a stainless-steel mesh filter with a pore size of 0.2 mm to remove coarse particles. The mixture was then suction-filtered through a 2 μm filter. Suction filtration was repeated with the addition of acetone and re-dispersion was performed using Handy Sonic UH-50 (SMT CO., LTD, Tokyo, Japan) until no clogging occurred; the filter was replaced with a 0.2 μm filter and the filtrate was suction-filtered. The 0.2 μm filter was collected and vacuum-dried for 30 min. The dried 0.2 μm filter was then transferred to a beaker, followed by the addition of t-butanol, and ultrasonic vibration was used to separate particles from the 0.2 μm filter. Thereafter, t-butanol containing the separated particles was collected in a test tube. The test tubes were chilled in a freezer for approximately 5 min, and the particles were collected using a UT-1010 lyophilizer (EYELA, Tokyo, Japan). To ensure the chemical integrity of the nanoparticles during preparation, additive-free plastics were used as starting materials. After each preparation, the collected particles were routinely analyzed using ATR-IR spectroscopy as part of quality control. These analyses confirmed that no degradation or chemical alteration occurred during the entire preparation process.

2.4. Microscopic imaging

The PE/PVC samples were transferred to dedicated 96-well plates and photographed using the CellVoyager 8000 (Yokogawa Inc., Tokyo, Japan). Images were captured using a Hamamatsu ORCA-Flash4.0 sCMOS camera equipped with a 4 × dry objective, an LED lamp, and a 525/50 nm bandpass emission filter.

2.5. Scanning electron microscopy (SEM) imaging

SEM measurements were performed using a field-emission scanning electron microscope (SU6600; Hitachi High-Tech, Tokyo, Japan). The sample was fixed to a sample stand with a carbon tape, and images were taken at an acceleration voltage of 15 kV (PE-NP/dPE-NP) or 10 kV (PVC-NP/dPVC-NP).

2.6. Particle size distribution measurement by dynamic light scattering (DLS)

Zetasizer Nano S (Malvern Panalytical, Malvern, UK) was used for DLS measurements; PE-NP was dispersed in 50 % ethanol (MilliQ as solvent) at 1 mg/mL and PVC-NP in MilliQ at 1 mg/mL. The particles were dispersed for 15 min using an ultrasonic cleaner and then transferred to a polystyrene cell for measurements.

2.7. Cell culture

In this study, the mouse macrophage-like cell line RAW264.7 (American Type Culture Collection (ATCC), Manassas, VA, USA) was used. RAW264.7 cells were cultured in Dulbecco's Modified Eagle Medium (high glucose) supplemented with L-glutamine and phenol red (Wako, Osaka, Japan), 10 % fetal bovine serum (FBS, Biosera, Nuaille, France), and 1 % (v/v) penicillin-streptomycin-amphotericin B suspension (FUJIFILM Wako Pure Chemical, Osaka, Japan) and maintained at 37 °C at 5 % CO2 and > 95 % humidity. Mycoplasma tests were routinely performed using a commercially available EZ-PCR Mycoplasma Detection Kit (Biological Industries, Beit-Haemek, Israel).

2.8. RNA Sequencing

Bulk RNA-seq analysis was performed at the NGS Core Facility of the Genome Information Research Center, Research Institute for Microbial Diseases, The University of Osaka. Genes with fragments per kilobase of exon per million mapped reads (FPKM) values below 0.5 were excluded from downstream analysis. Scatterplots and heatmaps were generated in RStudio (team, 2025) using the ggplot2 (Wickham, 2016) and pheatmap (Kolde, 2010) packages. For pathway analysis, genes with a $\log_2$ fold change greater than 1 in the dPE-MP group compared with the NT group were analyzed using the Enrichr web tool (Xie et al., 2021). Pathways from the *KEGG 2021 Human*, *BioPlanet 2019*, and *MSigDB Hallmark 2020* databases were evaluated. Expression changes in genes associated with Ferroptosis (KEGG 2021 Human) and the Reactive Oxygen Species Pathway (MSigDB Hallmark 2020) were visualized as heatmaps.

2.9. Annexin V assay

To analyze cell death type, annexin V (Bio Legend, San Diego, CA, USA) staining was performed, according to the manufacturer's instructions. Briefly, RAW264.7 cells were incubated with non-degraded/degraded PE/PVC. Carboxymethyl cellulose CMC (0.001 %) was used as a dispersant of PE in the medium. Staurosporine (200 nM; Cayman Chemical) was used as the positive control. After 24 h of incubation, cells were harvested via trypsinization. Subsequently, 100 μL of cell suspension containing approximately 1×10^5 cells were resuspended in 5 μL of 90 μg/mL FITC Annexin V and 10 μL of 1.25 mg/mL propidium iodide (Sigma Aldrich, St. Louis, MO, USA). This was followed by 15 min of incubation at room temperature in dark. Then, cells were resuspended with 400 μL of binding buffer, which contained 2 % FBS and 0.05 % sodium azide (Wako) in phosphate-buffered saline. Stained cells were analyzed by flow cytometry using MACSQuantX (Miltenyi Biotec, Bergisch Gladbach, Germany). Note that significance was assessed in each cell population using two-way ANOVA followed by Tukey's method.

2.10. Cell viability assay

Cell viability was measured using the 3-(4,5-dimethylthiazol-2-yl)-2,5-diphenyl tetrazolium bromide (MTT) assay (Tokyo Chemical Industry, Tokyo, Japan), according to the manufacturer's instructions.

2.11. Reactive oxygen species (ROS) assay

Intracellular ROS was measured using CM-H2DCFDA (General Oxidative Stress Indicator) (Thermo Fisher Scientific), according to the manufacturer's instructions. Stained cells were analyzed by flow cytometry using MACSQuantX (Miltenyi Biotec).

2.12. Lipid peroxidation measurement

Lipid peroxidation was measured using BODIPY™ 581/591 C11 (Thermo Fisher Scientific, Waltham, MA, USA). Briefly, after incubation, cells were stained with BODIPY™ 581/591 C11 and analyzed by flow cytometry using a MACSQuant X flow cytometer (Miltenyi Biotec).

2.13. Statistical analysis

Statistical analyses were performed using GraphPad Prism 9 for MacOS (version 9.5.0).

Results are presented as means ± SD. A one- or two-way analysis of variance with Tukey's multiple comparison test was used to determine statistically significant difference among groups (ns, not significant; *P < 0.05; **P < 0.01; ***P < 0.001; ****P < 0.0001).

3. Results

3.1. RNA-seq analysis revealed degraded MP alters ferroptosis-related gene signature

In this study, PE was selected as the model polymer because of its high global production rate (Geyer et al., 2017a). PE-MP and dPE-MP with average diameters of 231.4 and 231.9 μm, respectively (Ikuno

et al., 2024b), both having a fragment-like shape (Supplementary Fig. 1 A), were used. Surface properties were evaluated using ATR-IR analysis, which confirmed the introduction of carbonyl groups onto the surface (Supplementary Fig. 1B). Additional characteristics of dPE-MPs have been described previously (Manabe et al., 2024; Ikuno et al., 2024b); dPE-MPs, generated through VUV exposure, promote lysosomal deregulated cell death (Manabe et al., 2024). However, the precise molecular dynamics and the types of cell death remain unexplored. To address these questions, a transcriptomic analysis was conducted to evaluate the effects of PE-MP and dPE-MP exposure using RAW264.7 macrophage-like cells. The concentration of both PE-MP and dPE-MP was selected as 25 mg/mL based on previous findings in which dPE-MP exhibited slight cytotoxicity at this level. After 24 h of exposure, RNA-seq was performed to investigate cellular responses. The scatter plots (Fig. 1A) and heatmap (Fig. 1B) clearly indicate significant changes in gene expression in cells exposed to dPE-MP compared with those exposed to PE-MP. To investigate molecular expression changes following dPE-MP exposure, pathway analysis was conducted using genes with $\log_2$ fold-change values greater than 1 in the dPE-MP group compared with the NT group. The bubble plot revealed enrichment of multiple pathways, including xenobiotic metabolism, ferroptosis, fatty acid degradation, peroxisome, AMPK signaling, glutathione metabolism, TGF-β regulation of ECM, and ROS (Fig. 1C). These results indicate that dPE-MP elicits diverse cellular responses. For example, glutathione metabolism is linked to antioxidant defense (Kankaya et al., 2023), while xenobiotic metabolism involves cytochrome P450 enzymes (Esteves et al., 2021). Importantly, ferroptosis, which is a recently discovered form of programmed cell death induced by the iron-dependent accumulation of lipid peroxides (Dixon et al., 2012), and its related pathways, including glutathione metabolism, ROS regulation, and fatty acid degradation were enriched, supporting ferroptosis as a potential mechanism of cell death. To further clarify transcriptional changes in dPE-MP-treated cells, RNA-seq data were specifically examined for genes included in the Ferroptosis pathway (KEGG 2021 Human) and the Reactive Oxygen Species Pathway (MSigDB Hallmark 2020) (Fig. 1D). This analysis demonstrated that many genes associated with ferroptosis and ROS regulation were upregulated in the dPE-MP-treated groups, further supporting the involvement of ferroptosis-related processes in the cellular response to degraded PE-MPs. Collectively, transcriptomic data revealed that dPE-MP exposure altered ferroptosis related gene signature as well as other diverse cellular responses in RAW264.7 cells.

3.2. dPE-MP exposure promotes lipid peroxidation and ROS accumulation

Since the transcriptomics data suggested that dPE-MP altered gene expression related to ferroptosis and lipid peroxidation and ROS are key characteristics of ferroptosis (Endale et al., 2023), flow cytometry was performed to evaluate ROS accumulation and lipid peroxidation following dPE-MP treatment. The results revealed that both ROS and lipid peroxidation levels were significantly increased in the dPE-MP-treated group compared with the non-treated and PE-MP-treated groups (Figs. 2A and 2B). Collectively, our results indicated that dPE-MP treatment induced lipid peroxidation and ROS accumulation in RAW264.7 cells.

3.3. dPVC-MP promotes lipid peroxidation in RAW264.7 cells

Previous results demonstrated that dPE-MP induces cell death and lipid peroxide accumulation in RAW264.7 cells. Next, to determine whether dPE-MP-induced cell death mechanism is specific to PE or consistent across different polymer types, attention was next directed to another representative polymer material. PVC was selected for this purpose due to its widespread presence in the environment (Geyer et al., 2017b) and its documented association with human diseases (Marfella et al., 2024). PVC-MP used in this study was confirmed to be approximately 100 μm in size, having a fragment-like shape (Supplementary Fig. 2A). Furthermore, it was subjected to VUV radiation at a wavelength of 172 nm, replicating the treatment used for dPE-MP, to produce environmentally weathered PVC-MP. The surface characteristics of degraded PVC-MP (dPVC-MP) were analyzed using ATR-IR spectroscopy. The ATR-IR spectra revealed the presence of a peak at approximately 1426 cm^{-1}, corresponding to CH_2 bending vibrations, and the appearance of a C═O stretching band at 1724 cm^{-1} following VUV exposure (Supplementary Fig. 2B), which exhibits a similar pattern to previously reported values in environmental scenarios (Maddison et al., 2023). In our previous study, Annexin V and PI staining confirmed that dPE-MP induces programmed cell death (Manabe et al., 2024). Thus, in this study, Annexin V and PI staining along with flow cytometry were employed to assess the effect of PVC-MP and dPVC-MP. The results demonstrated a significant increase in Annexin V-positive cells following dPVC-MP treatment, whereas no such increase was observed with PVC-MP treatment (Fig. 3A). To test the possibility of lipid peroxidation in dPVC-MP-induced cell death, flow cytometric analysis was conducted in the PVC-MP- and dPVC-MP-treated cells. Flow cytometric analysis revealed an upregulation in dPVC-MP-treated cells (Fig. 3B). Therefore, dPVC-MP may induce cell death and lipid peroxide accumulation in RAW264.7 cells.

3.4. Degraded PE and PVC nanoplastics trigger lipid peroxidation and cell death

Since degraded MPs derived from different polymers, PE and PVC, were demonstrated to induce cell death and lipid peroxidation, subsequent investigations focused on evaluating the effects of smaller particles, specifically NP, on cell death induction and determining whether their capacity to induce lipid peroxide accumulation was exclusive to their degraded forms. NP are defined as plastic particles smaller than 1 μm, and their biological impact is of concern because of their small size (Shukla et al., 2025). PE-NP and PVC-NP were prepared using a previously established precipitation-based method (Tanaka et al., 2021) (Supplementary Fig. 3). Both PE-NP and PVC-NP, with or without degradation, exhibited a spherical shape (Supplementary Fig. 3A, 3D). Furthermore, the size range was determined to be within 300–600 nm (Supplementary Fig. 3B, 3E), consistent with the definition of NPs, characterized by dimensions less than 1 μm. Additionally, to mimic the surface oxidation observed in environmentally weathered MNPs, VUV treatment was applied to induce surface degradation in both PE-NP and PVC-NP, resulting in degraded PE-NP (dPE-NP) and degraded PVC-NP (dPVC-NP), respectively (Supplementary Fig. 3C, 3F). Cytotoxicity of PE-NP and dPE-NP was initially assessed via the MTT assay. While PE-NP exhibited no cytotoxic effects on RAW264.7 cells, dPE-NP induced significant cytotoxicity after 24 h of exposure (Fig. 4A). To further investigate the potential involvement of lipid peroxidation, lipid peroxidation levels after NP exposure were examined. Flow cytometry analysis revealed a marked increase in lipid peroxidation in the dPE-NP-treated group compared with the untreated and PE-NP-treated groups (Fig. 4B). The effects of different types of polymer NPs were assessed using dPVC-NP with the same analytical methods. The MTT assay demonstrated that dPVC-NP treatment resulted in a significantly higher cytotoxicity than PVC-NP treatment in RAW264.7 cells (Fig. 4C). Additionally, dPVC-NP treatment led to a notable increase in lipid peroxidation (Fig. 4D), consistent with the effects observed after dPE-NP treatment.

4. Discussion

Lipid peroxidation was identified as a critical mechanism underlying the observed cytotoxicity in the present study. Although lipid peroxidation is widely recognized as a promoter of ferroptosis, which has been implicated in various pathological conditions (Li et al., 2020) including

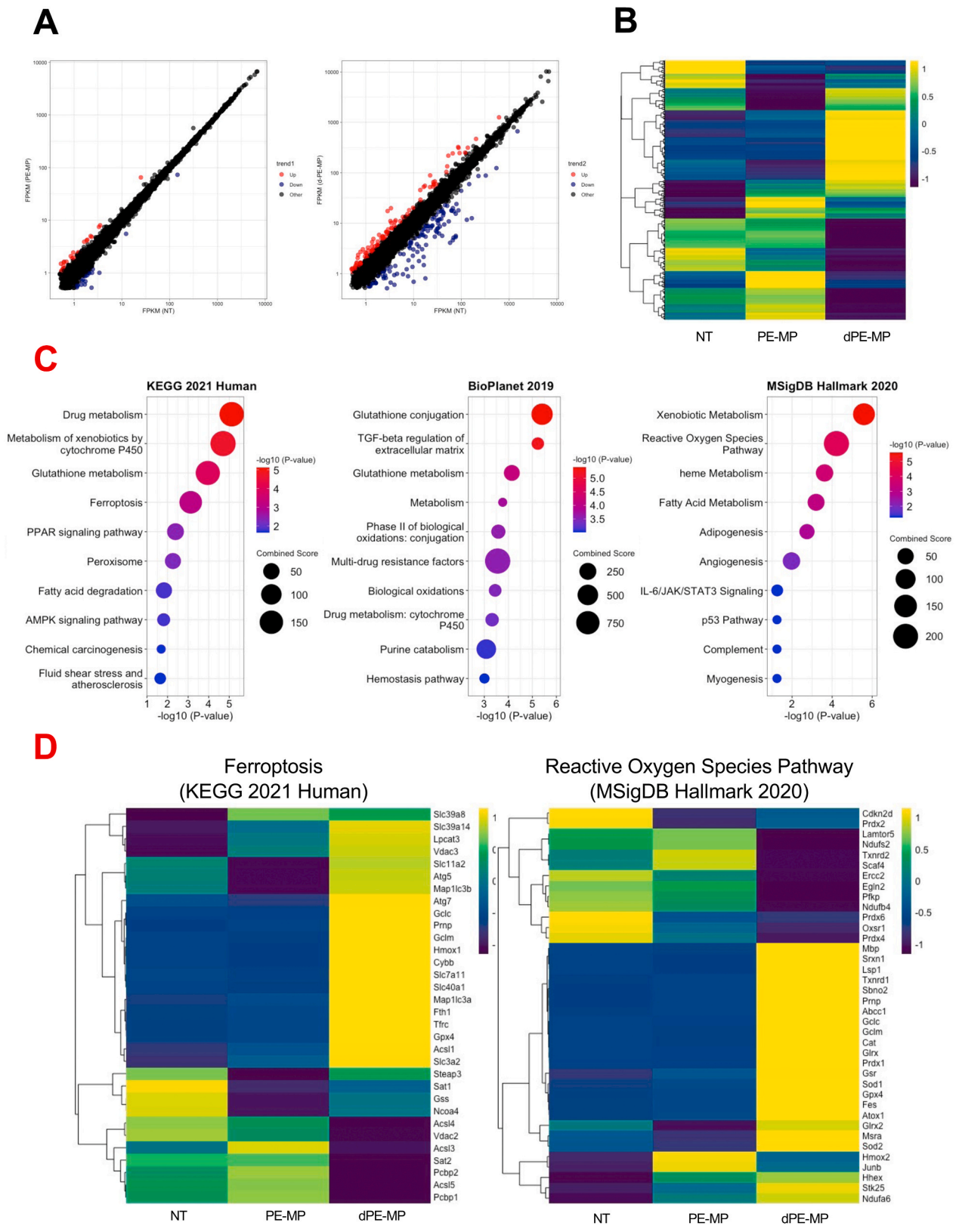

Fig. 1. Transcriptomic profiling of RAW264.7 cells exposed to PE-MP and dPE-MP. RAW264.7 cells were seeded in 6-well plates at a density of 2.0×10^5 cells per well and incubated for 24 h. The cell culture medium was then replaced with a medium containing 25 mg/mL of either non-degraded or degraded PE-MP, followed by incubation for 24 h. After incubation, the total RNA was extracted and subjected to RNA-seq analysis. Genes with FPKM values below 0.5 were excluded. (A) Scatter plots comparing NT (not treated) and PE-MP (left panel) and NT and dPE-MP (right panel). (B) Heatmap of the RNA-seq analysis comparing the NT, PE-MP, and dPE-MP groups. (C) Pathway enrichment analysis of 87 genes with a $\log_2$ fold change > 1 in the dPE-MP group compared with the NT group was performed using Enrichr (https://maayanlab.cloud/Enrichr/). Pathways from the KEGG 2021 Human, BioPlanet 2019, and MSigDB Hallmark 2020 databases were evaluated. (D) Heatmaps show expression changes in genes associated with Ferroptosis (KEGG 2021 Human) and the Reactive Oxygen Species Pathway (MSigDB Hallmark 2020).

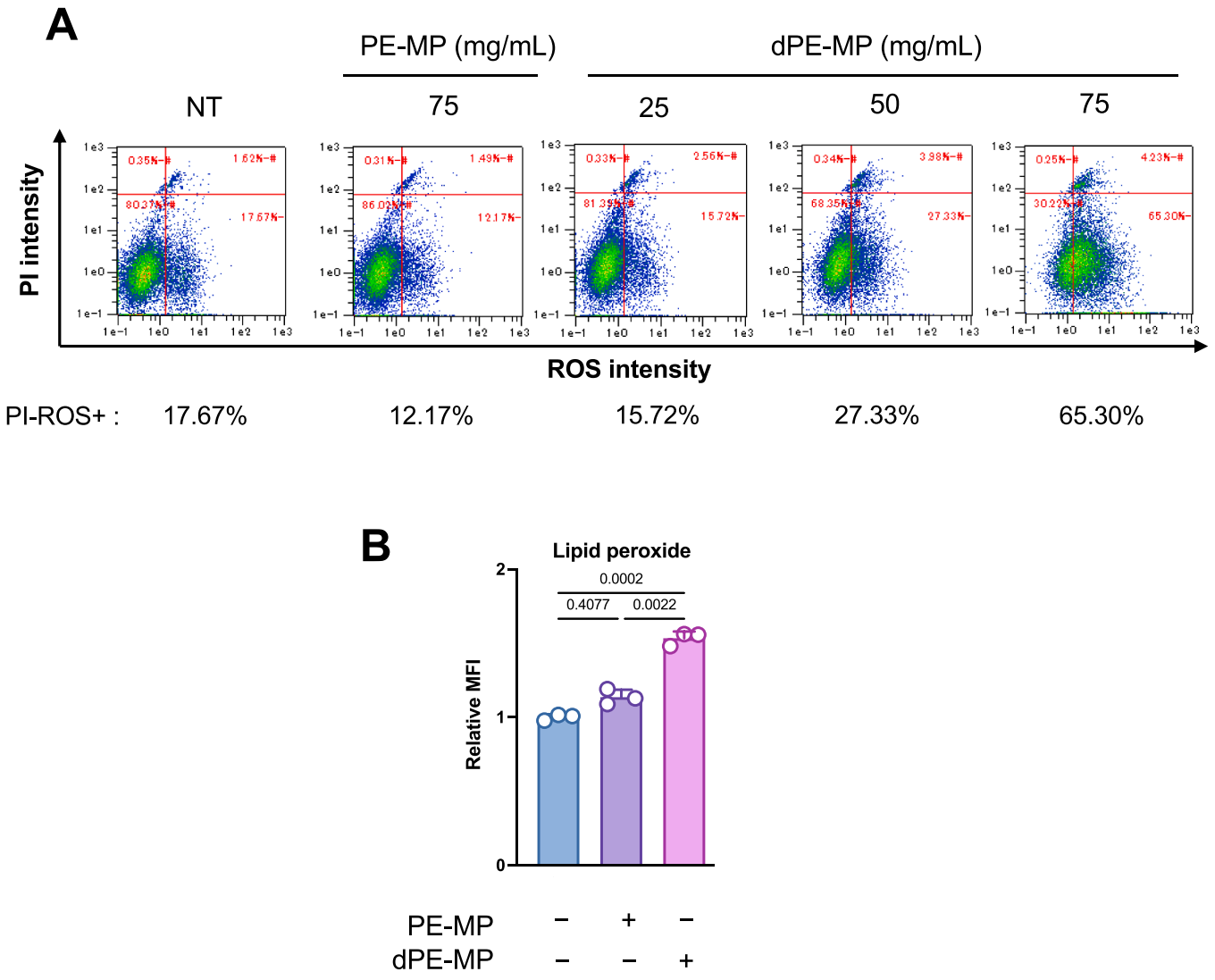

Fig. 2. Reactive oxygen species and lipid peroxidation accumulation in RAW264.7 cells exposed to dPE-MP. (A) RAW264.7 cells were seeded at 1×10^5 cells per well in 12-well plate and treated with non-degraded or degraded PE-MP of different concentrations (25, 50, and 75 mg/mL) for 8 h. After incubation, cells were stained with CM-H2DCFDA. After an hour of incubation, cells were analyzed using flow cytometry. The experiment was repeated twice with similar results. (B) RAW264.7 cells were seeded at 1×10^5 cells per well in a 12-well plate and treated with non-degraded or degraded PE-MP at a concentration of 25 mg/mL for 24 h. After incubation, cells were stained with BODIPY™ 581/591 C11 and analyzed using flow cytometry. The experiment was repeated twice with similar results. The bar graph represents means ± SD (n = 3). Note that significance was assessed using one way ANOVA followed by Tukey's method.

cardiovascular diseases, neurodegenerative disorders, and cancer (Yan et al., 2021; Wang et al., 2022), a limitation of this study is the absence of direct evidence demonstrating a causal link between ferroptosis and the observed lipid peroxidation. In this regard, the measurement of intracellular ferrous iron is an essential parameter for determining whether lipid peroxidation is specifically induced by iron accumulation. Additionally, lipid peroxidation itself, regardless of its association with ferroptosis, has been linked to disease processes such as neurological dysfunction and ischemia-reperfusion injury (Zheng et al., 2024). While further research is required to fully elucidate the relationship between MNP exposure and disease initiation *in vivo*, it is also necessary to investigate whether similar responses occur in non-immune cell types *in vitro*, as well as to clarify the *in vivo* biodistribution of the tested samples, particularly their potential to reach the brain or circulate in the bloodstream. Despite these limitations, our findings contribute to the existing literature by highlighting the role of lipid peroxidation in cellular responses to MNPs. Interestingly, our results demonstrated that the observed phenomena of lipid peroxidation and cytotoxicity were consistent across various polymer types, including PE and PVC. Despite the structural differences between these polymers (Bule Možar et al., 2023), they induced similar cellular responses (see Fig. 4A, B for PE and Fig. 4C, D for PVC), suggesting that this phenotype may represent a general characteristic of MNPs. In addition, transcriptomic analysis revealed that dPE-MP exposure activated pathways other than ferroptosis (Fig. 1C), implying that multiple cellular responses may be triggered in parallel. Therefore, assessing whether ferroptosis and other related responses are also induced by different polymer types will be critical for advancing our understanding of the diverse cellular responses of MNPs. To further validate this hypothesis, additional studies involving other polymer types such as PS, polypropylene (PP), and polyethylene terephthalate (PET) are needed.

In this study, environmentally relevant MNPs were prepared, and their cytotoxic effects and underlying mechanisms were investigated *in vitro*. While recent studies have predominantly focused on PS particles (Thompson et al., 2024; De Ruijter et al., 2020), they often overlook the influence of environmental weathering (Lim, 2021b). Among various physicochemical properties, this study showed that surface-degraded MNPs exhibited significantly greater cytotoxicity compared to their

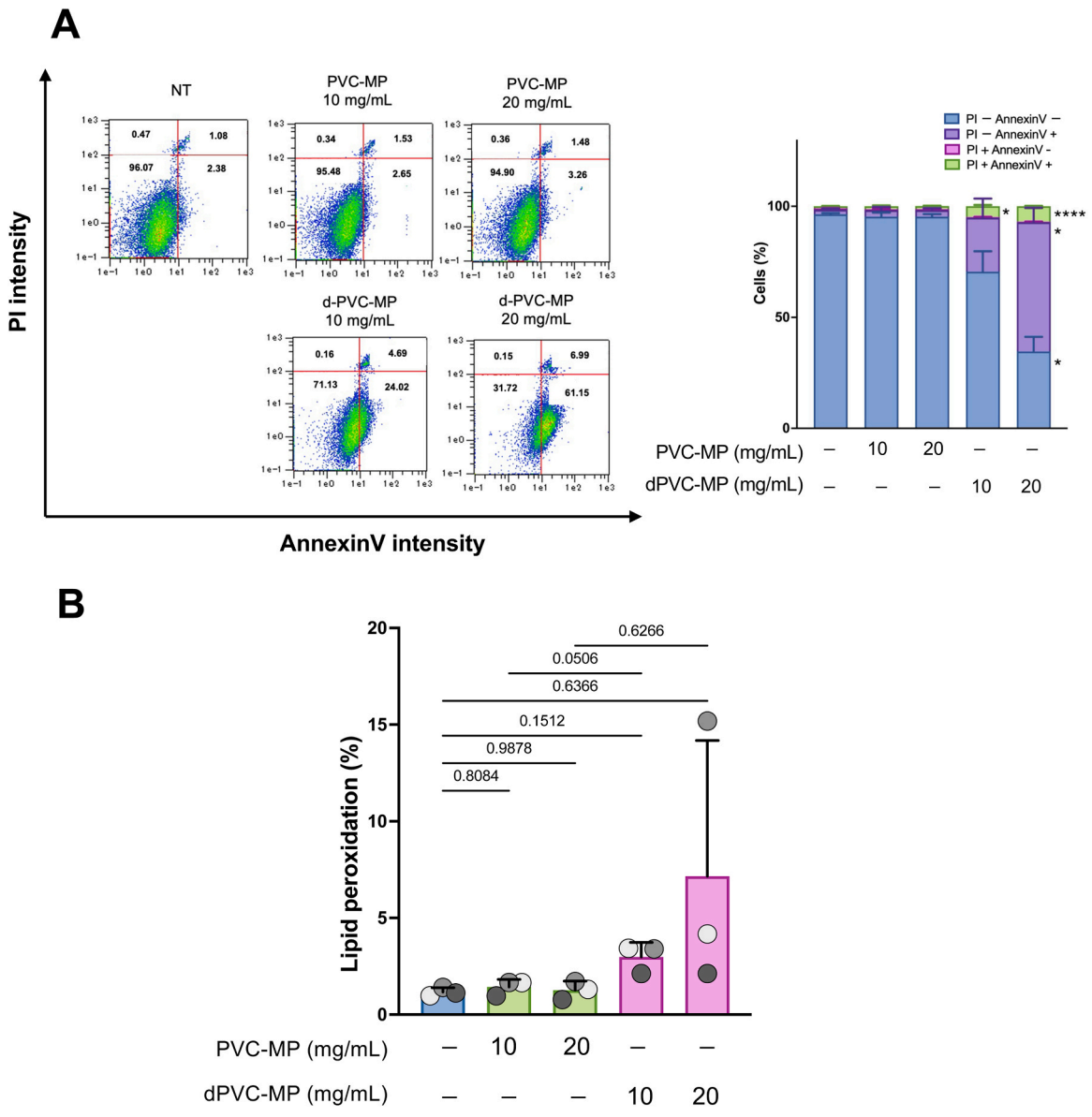

Fig. 3. Effect of PVC-MP/dPVC-MP on cell death and lipid peroxidation. (A) RAW264.7 cells were seeded in 12-well plates at a density of 5.0×10^4 cells per well and incubated for 24 h. The cell culture medium was then replaced by 800 μL of a medium containing different concentrations (10 and 20 mg/mL) of non-degraded or degraded PVC-MP and incubated for 24 h. Annexin V level and PI incorporation was determined using flow cytometry. Histogram at the right panel represent the cell population of PI+ /Annexin V+ , PI−/Annexin V+ , PI+ /Annexin V−, and PI−/Annexin V− in RAW264.7 cells. (B) RAW264.7 cells were seeded at 1×10^5 cells per well in a 12-well plate and treated with non-degraded or degraded PVC-MP at different concentrations of 10 and 20 mg/mL for 24 h. After incubation, cells were stained with BODIPY™ 581/591 C11 and analyzed using flow cytometry. Data are presented as the mean ± SD from three independent experiments.

non-degraded counterparts. The degradation method employed in this study has previously been shown to produce particles with physicochemical characteristics similar to those found in environmental samples, as demonstrated in our earlier work (Ikuno et al., 2024a). These findings highlight the importance of using environmentally simulated MNPs when evaluating their biological effects. Particle size was also found to play a significant role in toxicity. While the evaluation methods for dPVC-MPs and dPVC-NPs differ and must be taken into consideration, dPVC-MPs induced slight cell death at 10 mg/mL (Fig. 3A), whereas dPVC-NPs caused severe cytotoxicity at the same concentration (Fig. 4C). Although further studies using size-controlled samples and consistent evaluation methods are necessary, this highlights the importance of size in determining the biological impact of MPs/NPs. PVC used in this study is a chlorine-containing polymer, making it more susceptible to degradation VUV irradiation compared to PE. Upon VUV irradiation, PVC undergoes oxidation initiated by the cleavage of C-Cl bonds and polyene formation due to HCl elimination (Shi et al., 2008). Given these degradation pathways, PVC is less stable under light exposure compared to PE. The fact that d-PVC, which is more prone to degradation than PE and possesses distinct functional groups, elicited similar cellular responses is a particularly intriguing finding. Future studies should further explore this phenomenon using a broader range of polymer materials.

Previous studies have employed PS-NPs with a smooth surface (Thompson et al., 2024; De Ruijter et al., 2020; Rozman et al., 2021); however, our findings from the current study indicate that using only smooth PS-NPs is insufficient to fully capture the complexity of toxicity mechanisms. The influence of particle shape and surface properties on toxicity has become evident and remains an intriguing area for further investigation (Lim, 2021b).

In this study, the acute phase of toxicity was investigated using relatively high concentrations of MNPs, which may exceed those

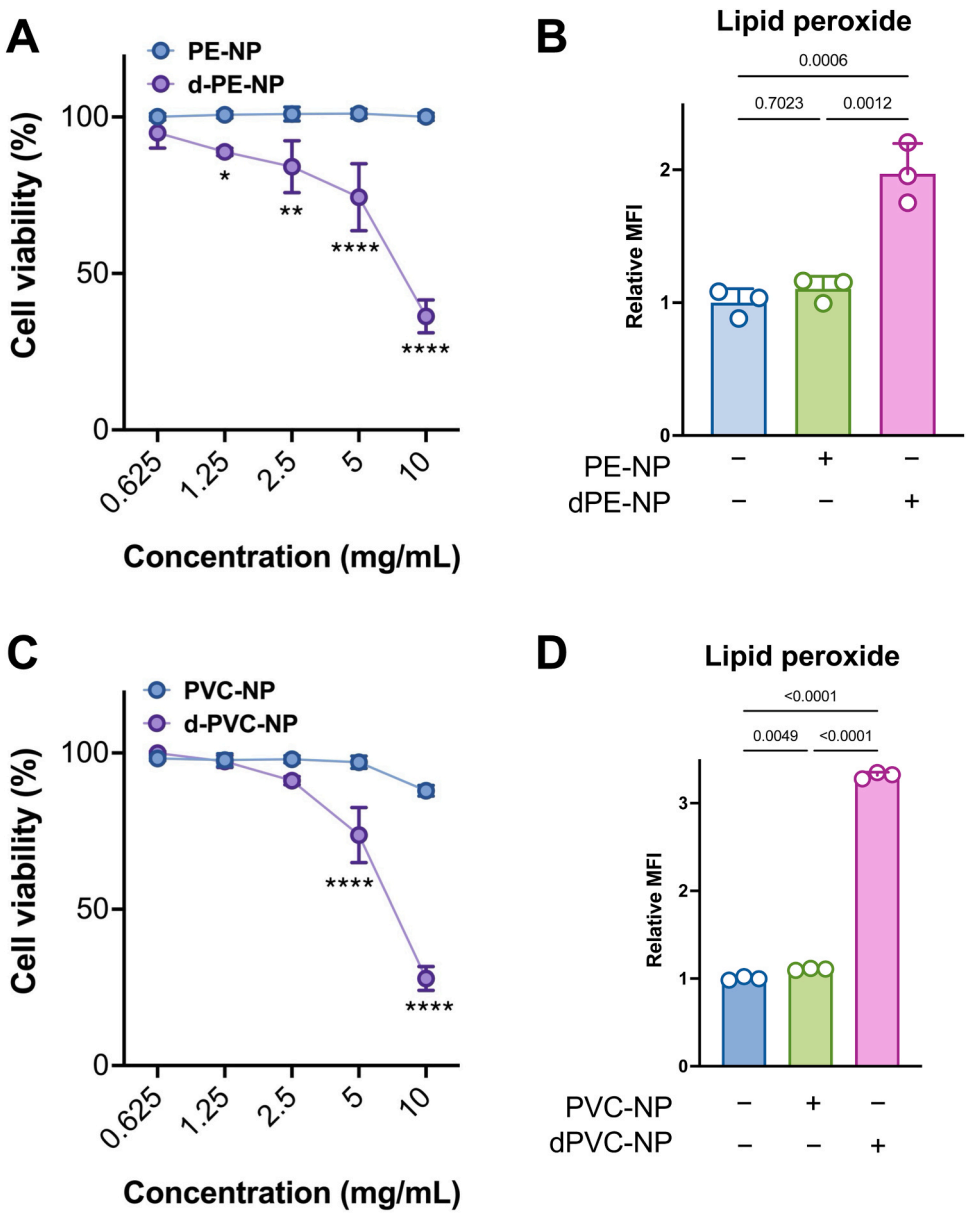

Fig. 4. Effect of PE-NP/dPE-NP and PVC-NP/dPVC-NP on cell death and lipid peroxidation. (A) RAW264.7 cells were seeded at 1×10^4 cells per well in a 96-well plate and incubated for 24 h. After incubation, cells were treated with non-degraded or degraded PE-NP at different concentrations for 24 h. Cell viability was determined by MTT assay. The graph represents means ± SD (n = 3). The experiment was repeated with similar results. (B) RAW264.7 cells were seeded at 1×10^5 cells per well in a 12-well plate and treated with non-degraded or degraded PE-NP at a concentration of 2.5 mg/mL for 24 h. After incubation, cells were stained with BODIPY™ 581/591 C11 and analyzed using flow cytometry. The bar graph represents means ± SD (n = 3). The experiment was repeated with similar results. (C) RAW264.7 cells were seeded at 1×10^4 cells per well in a 96-well plate and incubated for 24 h. After incubation, cells were treated with non-degraded or degraded PVC-NP at different concentrations for 24 h. Cell viability was determined using MTT assay. The graph represents means ± SD (n = 3). The experiment was repeated with similar results. (D) RAW264.7 cells were seeded at 1×10^5 cells per well in a 12-well plate and treated with non-degraded or degraded PVC-NP at a concentration of 1.25 mg/mL for 24 h. After incubation, cells were stained with BODIPY™ 581/591 C11 and analyzed using flow cytometry. The bar graph represents means ± SD (n = 3) The experiment was repeated with similar results.

typically encountered in the environment. Our primary objective was to investigate cellular responses within the acute exposure timeframe (up to 24 h). Given that VUV degradation may have caused particle fragmentation, resulting in the formation of very small particles, or monomers (Du et al., 2023), it is possible that only a small portion of the total particle population contributed to the observed cellular effects, such as cell death. While the use of high concentrations in acute exposure scenarios enabled us to elucidate fundamental mechanisms of toxicity, future experiments employing prolonged exposure to lower environmentally relevant concentrations are warranted to better simulate real-world scenarios.

To capture the expected temporal progression of cellular responses, ROS was measured after short-term exposure (8 h), lipid peroxidation at the mid-point of the acute phase (16 h), and cell death at 24 h. ROS generation typically occurs early, followed by lipid peroxidation (Murphy et al., 2022), which can ultimately result in cell death. Each response was therefore assessed at a distinct time point reflecting this progression. Although genes associated with ferroptosis were differentially expressed after 24 h of exposure, ROS was not detectable at 8 h, indicating that gene expression changes related to oxidative stress and lipid peroxidation may require longer exposure durations. Gene expression is also known to be dynamically regulated and influenced by

exposure concentration (Pascual-Ahuir et al., 2020). To overcome these limitations, future studies should incorporate time-resolved phenotypic measurements alongside transcriptomic analyses to better characterize the dynamics of the cellular response.

As a part of this study, MNP samples were developed using various polymer types and surface modifications (Supplementary Fig. 1, 2, and 3) specifically tailored to meet the objectives of the experiment. This study serves as a foundation for the future development of samples that better reflect the physicochemical properties of environmental micro- and nanoplastics. Such advancements are expected to enhance our understanding of cellular and biological responses upon exposure to these particles. Moreover, these findings have broader implications for environmental security and sustainable development. The demonstrated cytotoxic effects of environmentally relevant, surface-degraded MNPs emphasize the urgent need for preventive strategies to reduce plastic pollution and its downstream impacts on human and ecological health. A better understanding of the mechanisms underlying MNP toxicity supports the development of more accurate risk assessments and informs policy decisions aimed at improving waste management practices, minimizing the environmental release of plastics, and promoting the use of safer, biodegradable alternatives. In this context, the present research contributes not only to the scientific understanding of MNP hazards but also to broader efforts aimed at protecting environmental integrity and public health.

5. Conclusions

This study demonstrated that surface degradation enhances the cytotoxicity of MNPs, with lipid peroxidation identified as a key mechanism underlying the observed effects. Consistent cellular responses across different polymer types, such as PE and PVC, suggest that surface properties induced by environmental degradation play a central role in toxicity. The use of VUV irradiation enabled the preparation of environmentally relevant MNPs, reinforcing the importance of simulating real-world particle properties in toxicity assessments. Although a limitation of this study is the use of relatively high MNP concentrations, this approach was essential for investigating acute-phase cellular responses and identifying fundamental toxicity mechanisms within a short exposure timeframe. To build on these findings, future studies employing chronic, low-dose exposure models will be crucial for providing a more comprehensive understanding of the long-term biological impacts of environmentally degraded MNPs.

Data statement

All data analyzed in this study are included in the manuscript or supplementary information files.

CRediT authorship contribution statement

Kazuma Higashisaka: Writing – review & editing, Supervision. **Yasuo Tsutsumi:** Writing – review & editing, Supervision, Project administration, Funding acquisition, Conceptualization. **Sota Manabe:** Writing – review & editing, Writing – original draft, Visualization, Methodology, Investigation, Formal analysis, Data curation. **Mii Hokaku:** Writing – review & editing, Validation, Resources. **Phyo Bo Bo Aung:** Writing – review & editing, Validation, Resources. **Haruyasu Asahara:** Writing – review & editing, Validation, Resources. **Yuya Haga:** Writing – review & editing, Writing – original draft, Project administration, Methodology, Investigation, Formal analysis, Conceptualization. **Hirofumi Tsujino:** Writing – review & editing, Conceptualization. **Yudai Ikuno:** Writing – review & editing, Validation. **Wakaba Idehara:** Writing – review & editing, Validation.

Funding

This work was supported by the Environment Research and Technology Development Fund (JPMEERF20241003) of the Environmental Restoration and Conservation Agency provided by the Ministry of the Environment of Japan, Japan Society for the Promotion of Science (Grant Number 21K19336), Japan Ministry of Health, Labor and Welfare (Grant Number JPMH21447937), and the Sumitomo Foundation for Environmental Research Projects.

Declaration of Competing Interest

The authors declare that they have no known competing financial interests or personal relationships that could have appeared to influence the work reported in this paper.

Acknowledgements

We acknowledge the NGS core facility at the Research Institute for Microbial Diseases of The University of Osaka for the sequencing and data analysis. This research was partially supported by the Research Support Project for Life Science and Drug Discovery (Basis for Supporting Innovative Drug Discovery and Life Science Research) from AMED under Grant Number JP24ama121054. SEM analysis was performed using research equipment shared in the MEXT Project for Promoting the Public Utilization of Advanced Research Infrastructure (Program for Supporting the Construction of Core Facilities) Grant Number [JPMXS0441200024].

Appendix A. Supporting information

Supplementary data associated with this article can be found in the online version at doi:10.1016/j.ecoenv.2025.119030.

Data availability

Data will be made available on request.

References

A Review on Microplastics Migration from Sources Through Wastewater to the Environments, 2024. Classifications, Impacts and Removal Techniques. Emerging Contaminants and Associated Treatment Technologies. Springer Nature, Switzerland, Cham, pp. 675–703.

Agbasi, J.C., Egbueri, J.C., Pande, C.B., Khan, M.Y.A., Ighalo, J.O., Uwajingba, H.C., Abba, S.I., 2025. Review of the potential effects and remediation strategies of microplastic pollutants in drinking water sources. Anal. Lett. 58, 799–839. https://doi.org/10.1080/00032719.2024.2343366.

Alimi, O.S., Claveau-Mallet, D., Kurusu, R.S., Lapointe, M., Bayen, S., Tufenkji, N., 2022. Weathering pathways and protocols for environmentally relevant microplastics and nanoplastics: what are we missing? J. Hazard Mater. 423, 126955. https://doi.org/10.1016/j.jhazmat.2021.126955.

Almond, J., Sugumaar, P., Wenzel, M.N., Hill, G., Wallis, C., 2020. Determination of the carbonyl index of polyethylene and polypropylene using specified area under band methodology with ATR-FTIR spectroscopy. EPolym 20, 369–381. https://doi.org/10.1515/epoly-2020-0041.

Amato-Lourenço, L.F., Dantas, K.C., Júnior, G.R., Paes, V.R., Ando, R.A., De Oliveira Freitas, R., Da Costa, O.M.M.M., Rabelo, R.S., Soares Bispo, K.C., Carvalho-Oliveira, R., Mauad, T., 2024. Microplastics in the olfactory bulb of the human brain. JAMA Netw. Open 7, e2440018. https://doi.org/10.1001/jamanetworkopen.2024.40018.

Belioka, M.-P., Achilias, D.S., 2024. How plastic waste management affects the accumulation of microplastics in waters: a review for transport mechanisms and routes of microplastics in aquatic environments and a timeline for their fate and occurrence (past, present, and future). Water Emerg. Contam. Nanoplastics 3. https://doi.org/10.20517/wecn.2024.09.

Bule Možar, K., Miloloža, M., Martinjak, V., Cvetnić, M., Kušić, H., Bolanča, T., Kučić Grgić, D., Ukić, Š., 2023. Potential of advanced oxidation as pretreatment for microplastics biodegradation. Separations 10, 132. https://doi.org/10.3390/separations10020132.

De Ruijter, V.N., Redondo-Hasselerharm, P.E., Gouin, T., Koelmans, A.A., 2020. Quality criteria for microplastic effect studies in the context of risk assessment: a critical review. Environ. Sci. Technol. 54, 11692–11705. https://doi.org/10.1021/acs.est.0c03057.

Dixon, S.J., Lemberg, K.M., Lamprecht, M.R., Skouta, R., Zaitsev, E.M., Gleason, C.E., Patel, D.N., Bauer, A.J., Cantley, A.M., Yang, W.S., Morrison, B., Stockwell, B.R., 2012. Ferroptosis: an Iron-Dependent form of nonapoptotic cell death. Cell 149, 1060–1072. https://doi.org/10.1016/j.cell.2012.03.042.

Du, Z., Li, G., Ding, S., Song, W., Zhang, M., Jia, R., Chu, W., 2023. Effects of UV-based oxidation processes on the degradation of microplastic: fragmentation, organic matter release, toxicity and disinfection byproduct formation. Water Res. 237, 119983. https://doi.org/10.1016/j.watres.2023.119983.

Endale, H.T., Tesfaye, W., Mengstie, T.A., 2023. ROS induced lipid peroxidation and their role in ferroptosis. Front Cell Dev. Biol. 11, 1226044. https://doi.org/10.3389/fcell.2023.1226044.

Esteves, F., Rueff, J., Kranendonk, M., 2021. The central role of cytochrome P450 in xenobiotic Metabolism—A brief review on a fascinating enzyme family. J. Xenobiotics 11, 94–114. https://doi.org/10.3390/jox11030007.

Geyer, R., Jambeck, J.R., Law, K.L., 2017a. Production, use, and fate of all plastics ever made. Sci. Adv. 3, e1700782. https://doi.org/10.1126/sciadv.1700782.

Geyer, R., Jambeck, J.R., Law, K.L., 2017b. Production, use, and fate of all plastics ever made. Sci. Adv. 3, e1700782. https://doi.org/10.1126/sciadv.1700782.

Gigault, J., Halle, A.T., Baudrimont, M., Pascal, P.-Y., Gauffre, F., Phi, T.-L., El Hadri, H., Grassl, B., Reynaud, S., 2018. Current opinion: what is a nanoplastic? Environ. Pollut. 235, 1030–1034. https://doi.org/10.1016/j.envpol.2018.01.024.

Ibrahim, Y.S., Tuan Anuar, S., Azmi, A.A., Wan Mohd Khalik, W.M.A., Lehata, S., Hamzah, S.R., Ismail, D., Ma, Z.F., Dzulkarnaen, A., Zakaria, Z., Mustaffa, N., Tuan Sharif, S.E., Lee, Y.Y., 2021. Detection of microplastics in human colectomy specimens. JGH Open 5, 116–121. https://doi.org/10.1002/jgh3.12457.

Ikuno, Y., Tsujino, H., Haga, Y., Asahara, H., Higashisaka, K., Tsutsumi, Y., 2023. Impact of degradation of polyethylene particles on their cytotoxicity. Microplastics 2, 192–201. https://doi.org/10.3390/microplastics2020015.

Ikuno, Y., Tsujino, H., Haga, Y., Manabe, S., Idehara, W., Hokaku, M., Asahara, H., Higashisaka, K., Tsutsumi, Y., 2024b. Polyethylene, whose surface has been modified by UV irradiation, induces cytotoxicity: a comparison with microplastics found in beaches. Ecotoxicol. Environ. Saf. 277, 116346. https://doi.org/10.1016/j.ecoenv.2024.116346.

Ikuno, Y., Tsujino, H., Haga, Y., Manabe, S., Idehara, W., Hokaku, M., Asahara, H., Higashisaka, K., Tsutsumi, Y., 2024a. Polyethylene, whose surface has been modified by UV irradiation, induces cytotoxicity: a comparison with microplastics found in beaches. Ecotoxicol. Environ. Saf. 277, 116346. https://doi.org/10.1016/j.ecoenv.2024.116346.

Jenner, L.C., Rotchell, J.M., Bennett, R.T., Cowen, M., Tentzeris, V., Sadofsky, L.R., 2022. Detection of microplastics in human lung tissue using μFTIR spectroscopy. Sci. Total Environ. 831, 154907. https://doi.org/10.1016/j.scitotenv.2022.154907.

Kankaya, S., Yavuz, F., Tari, A., Aygun, A.B., Gunes, E.G., Bektan Kanat, B., Ulugerger Avci, G., Yavuzer, H., Dincer, Y., 2023. Glutathione-related antioxidant defence, DNA damage, and DNA repair in patients suffering from post-COVID conditions. Mutagenesis 38, 216–226. https://doi.org/10.1093/mutage/gead021.

Karami, A., Golieskardi, A., Keong Choo, C., Larat, V., Galloway, T.S., Salamatinia, B., 2017. The presence of microplastics in commercial salts from different countries. Sci. Rep. 7, 46173. https://doi.org/10.1038/srep46173.

Koelmans, A.A., Mohamed Nor, N.H., Hermsen, E., Kooi, M., Mintenig, S.M., De France, J., 2019. Microplastics in freshwaters and drinking water: critical review and assessment of data quality. Water Res. 155, 410–422. https://doi.org/10.1016/j.watres.2019.02.054.

Kolde, R., 2010. pheatmap Pretty Heatmaps 1 (0), 13.

Kye, H., Kim, J., Ju, S., Lee, J., Lim, C., Yoon, Y., 2023. Microplastics in water systems: a review of their impacts on the environment and their potential hazards. Heliyon 9, e14359. https://doi.org/10.1016/j.heliyon.2023.e14359.

Lambert, S., Scherer, C., Wagner, M., 2017. Ecotoxicity testing of microplastics: considering the heterogeneity of physicochemical properties. Integr. Environ. Assess. Manag 13, 470–475. https://doi.org/10.1002/ieam.1901.

Leslie, H.A., Van Velzen, M.J.M., Brandsma, S.H., Vethaak, A.D., Garcia-Vallejo, J.J., Lamoree, M.H., 2022. Discovery and quantification of plastic particle pollution in human blood. Environ. Int. 163, 107199. https://doi.org/10.1016/j.envint.2022.107199.

Li, J., Cao, F., Yin, H., Huang, Z., Lin, Z., Mao, N., Sun, B., Wang, G., 2020. Ferroptosis: past, present and future. Cell Death Dis. 11, 88. https://doi.org/10.1038/s41419-020-2298-2.

Lim, X., 2021b. Microplastics are everywhere — but are they harmful? Nature 593, 22–25. https://doi.org/10.1038/d41586-021-01143-3.

Lim, X., 2021a. Microplastics are everywhere — but are they harmful? Nature 593, 22–25. https://doi.org/10.1038/d41586-021-01143-3.

Maddison, C., Sathish, C.I., Lakshmi, D., Wayne, O., Palanisami, T., 2023. An advanced analytical approach to assess the long-term degradation of microplastics in the marine environment. Npj Mater. Degrad. 7, 59. https://doi.org/10.1038/s41529-023-00377-y.

Manabe, S., Haga, Y., Tsujino, H., Ikuno, Y., Asahara, H., Higashisaka, K., Tsutsumi, Y., 2024. Treatment of polyethylene microplastics degraded by ultraviolet light irradiation causes lysosome-deregulated cell death. Sci. Rep. 14, 24008. https://doi.org/10.1038/s41598-024-74800-y.

Marfella, R., Prattichizzo, F., Sardu, C., Fulgenzi, G., Graciotti, L., Spadoni, T., D'Onofrio, N., Scisciola, L., La Grotta, R., Frigé, C., Pellegrini, V., Municinò, M., Siniscalchi, M., Spinetti, F., Vigliotti, G., Vecchione, C., Carrizzo, A., Accarino, G., Squillante, A., Spaziano, G., Mirra, D., Esposito, R., Altieri, S., Falco, G., Fenti, A., Galoppo, S., Canzano, S., Sasso, F.C., Matacchione, G., Olivieri, F., Ferraraccio, F., Panarese, I., Paolisso, P., Barbato, E., Lubritto, C., Balestrieri, M.L., Mauro, C., Caballero, A.E., Rajagopalan, S., Ceriello, A., D'Agostino, B., Iovino, P., Paolisso, G., 2024. Microplastics and nanoplastics in atheromas and cardiovascular events. N. Engl. J. Med. 390, 900–910. https://doi.org/10.1056/NEJMoa2309822.

Modeling of Microplastic Contamination Using Soft Computational Methods: Advances, Challenges, and Opportunities, 2024. In: Emerging Contaminants and Associated Treatment Technologies. Springer Nature Switzerland, Cham, pp 553–579.

Murphy, M.P., Bayir, H., Belousov, V., Chang, C.J., Davies, K.J.A., Davies, M.J., Dick, T. P., Finkel, T., Forman, H.J., Janssen-Heininger, Y., Gems, D., Kagan, V.E., Kalyanaraman, B., Larsson, N.-G., Milne, G.L., Nyström, T., Poulsen, H.E., Radi, R., Van Remmen, H., Schumacker, P.T., Thornalley, P.J., Toyokuni, S., Winterbourn, C. C., Yin, H., Halliwell, B., 2022. Guidelines for measuring reactive oxygen species and oxidative damage in cells and in vivo. Nat. Metab. 4, 651–662. https://doi.org/10.1038/s42255-022-00591-z.

Okoye, C.O., Addey, C.I., Oderinde, O., Okoro, J.O., Uwamungu, J.Y., Ikechukwu, C.K., Okeke, E.S., Ejeromedoghene, O., Odii, E.C., 2022. Toxic chemicals and persistent organic pollutants associated with Micro-and nanoplastics pollution. Chem. Eng. J. Adv. 11, 100310. https://doi.org/10.1016/j.ceja.2022.100310.

Pascual-Ahuir, A., Fita-Torró, J., Proft, M., 2020. Capturing and understanding the dynamics and heterogeneity of gene expression in the living cell. Int J. Mol. Sci. 21, 8278. https://doi.org/10.3390/ijms21218278.

Ragusa, A., Svelato, A., Santacroce, C., Catalano, P., Notarstefano, V., Carnevali, O., Papa, F., Rongioletti, M.C.A., Baiocco, F., Draghi, S., D'Amore, E., Rinaldo, D., Matta, M., Giorgini, E., 2021. Plasticenta: first evidence of microplastics in human placenta. Environ. Int. 146, 106274. https://doi.org/10.1016/j.envint.2020.106274.

Rozman, U., Turk, T., Skalar, T., Zupančič, M., Čelan Korošin, N., Marinšek, M., Olivero-Verbel, J., Kalčíková, G., 2021. An extensive characterization of various environmentally relevant microplastics – material properties, leaching and ecotoxicity testing. Sci. Total Environ. 773, 145576. https://doi.org/10.1016/j.scitotenv.2021.145576.

Shi, W., Zhang, J., Shi, X., Jiang, G., 2008. Different photodegradation processes of PVC with different average degrees of polymerization. J. Appl. Polym. Sci. 107, 528–540. https://doi.org/10.1002/app.25389.

Shukla, S., Khanna, S., Khanna, K., 2025. Unveiling the toxicity of micro-nanoplastics: a systematic exploration of understanding environmental and health implications. Toxicol. Rep. 14, 101844. https://doi.org/10.1016/j.toxrep.2024.101844.

Sources and Environmental Distribution of Microplastics in Nigeria, 2024. Emerging Contaminants and Associated Treatment Technologies. Springer Nature Switzerland, Cham, pp. 107–130.

Tanaka, K., Takahashi, Y., Kuramochi, H., Osako, M., Tanaka, S., Suzuki, G., 2021. Preparation of nanoscale particles of five major polymers as potential standards for the study of nanoplastics. Small 17, 2105781. https://doi.org/10.1002/smll.202105781.

team, Posit, 2025. RStudio: Integrated Development Environment for R..

The Nexus Between the Transport Mechanisms and Remediation Techniques of Microplastics, 2024. Emerging Contaminants and Associated Treatment Technologies. Springer Nature Switzerland, Cham, pp. 259–292.

Thompson, R.C., Courtene-Jones, W., Boucher, J., Pahl, S., Raubenheimer, K., Koelmans, A.A., 2024. Twenty years of microplastic pollution research—what have we learned? Science 386. https://doi.org/10.1126/science.adl2746.

Thompson, R.C., Olsen, Y., Mitchell, R.P., Davis, A., Rowland, S.J., John, A.W.G., McGonigle, D., Russell, A.E., 2004. Lost at sea: where is all the plastic? Science 304, 838–8318. https://doi.org/10.1126/science.1094559.

Toxicological Effects of Ingested Microplastics on Human Health, 2024. Emerging Contaminants and Associated Treatment Technologies. Springer Nature Switzerland, Cham, pp. 427–461.

Trainic, M., Flores, J.M., Pinkas, I., Pedrotti, M.L., Lombard, F., Bourdin, G., Gorsky, G., Boss, E., Rudich, Y., Vardi, A., Koren, I., 2020. Airborne microplastic particles detected in the remote marine atmosphere. Commun. Earth Environ. 1, 64. https://doi.org/10.1038/s43247-020-00061-y.

Wang, K., Chen, X.-Z., Wang, Y.-H., Cheng, X.-L., Zhao, Y., Zhou, L.-Y., Wang, K., 2022. Emerging roles of ferroptosis in cardiovascular diseases. Cell Death Discov. 8, 394. https://doi.org/10.1038/s41420-022-01183-2.

Wickham, H., 2016. Second edition. ggplot2: Elegant Graphics for Data analysis. Springer international publishing, Cham.

Xie, Z., Bailey, A., Kuleshov, M.V., Clarke, D.J.B., Evangelista, J.E., Jenkins, S.L., Lachmann, A., Wojciechowicz, M.L., Kropiwnicki, E., Jagodnik, K.M., Jeon, M., Ma'ayan, A., 2021. Gene set knowledge discovery with enrichr. Curr. Protoc. 1, e90. https://doi.org/10.1002/cpz1.90.

Yan, Z., Liu, Y., Zhang, T., Zhang, F., Ren, H., Zhang, Y., 2022. Analysis of microplastics in human feces reveals a correlation between fecal microplastics and inflammatory bowel disease status. Environ. Sci. Technol. 56, 414–421. https://doi.org/10.1021/acs.est.1c03924.

Yan, H., Zou, T., Tuo, Q., Xu, S., Li, H., Belaidi, A.A., Lei, P., 2021. Ferroptosis: mechanisms and links with diseases. Signal Transduct. Target Ther. 6, 49. https://doi.org/10.1038/s41392-020-00428-9.

Zheng, Y., Sun, J., Luo, Z., Li, Y., Huang, Y., 2024. Emerging mechanisms of lipid peroxidation in regulated cell death and its physiological implications. Cell Death Dis. 15. https://doi.org/10.1038/s41419-024-07244-x.